Western-diet consumption induces alteration of barrier function mechanisms in the ileum that correlates with metabolic endotoxemia in rats

Mathilde Guerville, Anaïs Leroy, Annaëlle Sinquin, Fabienne Laugerette, Marie-Caroline Michalski, Gaëlle Boudry

Western-diet consumption induces alteration of barrier function mechanisms in the ileum, that correlates with metabolic endotoxemia in rats.

Mathilde Guerville[1], Anaïs leroy[1], Annaëlle Sinquin[1], Fabienne Laugerette[2], Marie-Caroline Michalski[2] and Gaëlle Boudry[1]

[1] Institut Numecan INRA INSERM Université de Rennes 1, Domaine de la Prise, 35590 Saint-Gilles, France
[2] Univ-Lyon, CarMeN Laboratory, INRA U1397, Université Claude Bernard Lyon 1, Inserm U1060, INSA Lyon, F-69100, Villeurbanne, France

RUNNING TITLE: LPS handling in diet-induced metabolic endotoxemia

CORRESPONDING AUTHOR:
Dr Boudry Gaëlle
Institut Numecan INRA INSERM Université de Rennes 1
Domaine de la Prise
35590 Saint-Gilles
Tel: +33 (0)2 23 48 59 76
gaelle.boudry@ inra.fr

Abstract

Obesity and its related disorders have been associated to the presence in the blood of gut bacteria-derived lipopolysaccharides (LPS). However, the factors underlying this low-grade elevation in plasma LPS, so-called metabolic endotoxemia, are not fully elucidated. We aimed to investigate the effects of Western diet (WD) feeding on intestinal and hepatic LPS handling mechanisms in a rat model of diet-induced obesity (DIO). Rats were fed either a standard chow diet (C) or a Western Diet (WD, 45% fat) for 6 weeks. They were either fed *ad libitum* or pair-fed to match the caloric intake of Crats for the first week then fed *ad libitum* for the remaining 5 weeks. Six-week WD feeding led to a mild obese phenotype with increased adiposity and elevated serum LPS-binding protein (LBP) levels relative to C rats, irrespective of initial energy intake. Serum LPS was not different between dietary groups but exhibited strong variability. Disrupted ileal mucus secretion and decreased ileal Reg3-γ and -β gene expression along with high ileal permeability to LPS were observed in WD compared to C-fed rats. Ileal and caecal intestinal alkaline phosphatase (IAP) activity as well as Verrucomicrobia and Bifidobacterium caecal levels were increased in WD-fed rats compared to C-fed rats. WD consumption did not impact mRNA levels of LPS-handling hepatic enzymes. Correlation analysis revealed that ileal passage of LPS, IAP activity, Proteobacteria levels and hepatic aoah gene expression correlated with serum LPS and LBP, suggesting that ileal mucosal defense impairment induced by WD feeding contribute to metabolic endotoxemia.

Introduction

Obesity-associated metabolic disorders (type 2 diabetes, cardiovascular diseases and non-alcoholic fatty liver disease) are clearly related to chronic low-grade inflammation observed in obesity (28, 32). Although this obesity-associated low-grade inflammation is widely accepted, its etiology was not completely understood until Cani *et al* hypothesized that component from the gut microbiota, lipopolysaccharides (LPS), could be inflammatory triggering factors (12). Often referred to as endotoxins, LPS are constituents of the cell wall of Gram-negative bacteria present in the gut microbiota (14, 21). One of their components, the lipid A, is a pathogen associated molecular pattern (14, 21) recognized by host Toll-Like receptor 4 (TLR4). Binding of lipid A to TLR4 initiates signaling cascades resulting in the production of pro-inflammatory cytokines including Interleukine-1-β (IL-1β) or Tumor Necrosis Factor-α (TNF-α) (61). In the systemic circulation, LPS is transported by the LPS-binding protein (LBP), an acute phase protein exhibiting a high affinity to the lipid A moiety (63). In a series of experiments on genetically obese or diet-induced obese (DIO) mice, Cani *et al* described a condition of chronically elevated plasma LPS levels 5 times lower than during sepsis but significantly greater than in lean mice termed “metabolic endotoxemia” (12, 13). They demonstrated that experimental metabolic endotoxemia, performed with subcutaneous infusions of LPS in mice, induces obesity and metabolic disorders i.e. inflammation, weight gain and hepatic steatosis, similar to Western diet (WD) feeding (12). The relationship between metabolic endotoxemia and obesity-associated metabolic disorders has been confirmed in multiples animal and human studies (5, 11, 16, 17, 27, 34, 43, 48, 53, 55, 56, 75, 80). Some studies failed to show an increase in plasma LPS in obese animals (37), which might be due to initial microbiota composition (56). Moreover, because plasma levels of LPS are fluctuant due to circadian rhythm and LPS concentrations difficult to measure due to technical constraints (10), the use of plasma LBP as a long-term marker of hepatic LPS exposure and therefore of metabolic endotoxemia is now widely recognized.

65 The gut microbiota is the major source of LPS, with a rough estimation of 1 g of LPS within the gut
66 (25). In healthy conditions, multiple mechanisms occur at the intestinal level to keep LPS within the
67 gut lumen and avoid its presence into the systemic circulation. Numerous proteins e.g. mucus,
68 antimicrobial peptides (AMPs) or intestinal enzymes like intestinal alkaline phosphatase (IAP) are
69 secreted by epithelial cells into the lumen, ensuring primary line of defense against noxious stimulus,
70 including LPS (7, 25). In the small intestine, it is admitted that LPS mainly crosses the enterocytes
71 through the chylomicrons pathway after a lipid-rich meal (42). Conversely, in the large intestine or
72 during inter-prandial periods in the small intestine, the precise mechanisms by which LPS crosses
73 epithelial cells are unknown (25). Finally, if LPS crosses the intestine and spreads into the portal vein,
74 the liver is endowed with major detoxification processes through specific enzymes
75 (acyloxyaclyhydroxylase and alkaline phosphatase) or scavenger-receptor-mediated excretion into the
76 bile (25).

77 There are conflicting results regarding how the intestine adapts to western diet feeding, resulting in
78 metabolic endotoxemia. Changes in microbiota composition with lower diversity have been observed
79 (27); yet no consensus on the bacterial composition of WD-fed animals that could result in increased
80 quantity of lumen LPS has emerged so far. The impact of WD feeding on mucosal secreted factors
81 (mucus, AMPs, IAP) mechanisms is also controversial with either protective or deleterious effects on
82 mucosal barrier function (1, 5, 6, 27, 74). Furthermore, metabolic endotoxemia has been largely
83 associated with increased gut permeability. It has even been hypothesized to be the main cause of
84 elevated endotoxemia observed in DIO, based on parallel increase in *in vivo* permeability to
85 fluorescently-tagged small molecules and plasma LPS level (13, 17, 31, 52, 66). Yet, no study so far
86 has used tagged-LPS to investigate which portion(s) of the gut is/are more permeable to LPS in
87 conditions of metabolic endotoxemia. Likewise, WD feeding impacts on hepatic mechanisms of LPS
88 detoxification or disposal are currently overlooked. Therefore our primarily aim was to describe the
89 changes in intestinal (ileum and caecum) and hepatic LPS handling mechanisms in a rat model of
90 metabolic endotoxemia induced by 6 weeks of WD feeding. Because rodents switched to a WD
91 display a transient phase of overconsumption of calories during the first days of feeding (27, 77, 78),

we included a group of pair-fed animals fed the WD but with similar caloric intake than control animals the first days of feeding. Unexpectedly, some of these animals exhibited high variability in serum LPS levels and differences in intestinal physiology compared to *ad-libitum*-fed WD rats. Investigating the mechanisms by which these animals displayed such differences was beyond the scope of this study but we took advantage of this variability in the response of WD feeding to explore which mechanisms and in which section of the intestine could best explain the increased serum LBP and/or LPS observed in DIO.

Material and method

Animals

All experiments were performed in accordance with the European Union Guidelines for Animal Care and Use under file #APAFIS#903-2015061809202358V3. Male Wistar Rats (8-9 week old; 380 ± 25 g; Janvier Labs, Le Genest-Saint-Isle, France) were housed individually with a 12-h light/dark cycle and maintained at 22°C ± 2°C. They had free access to water and standard chow (Special Diets Services, Rat and Mouse N°3 Breeding, Witham, UK) during a 1-week acclimatization period prior to the diet intervention.

After acclimatization, rats were split into 4 weight-matched groups. Two groups of 6 rats were provided *ad libitum* access to either the standard chow diet (Cal) or a Western Diet (WDal) (D12451, Research Diets, New Brunswick, NJ, USA , fat 45% of total energy, 11% gm cellulose, 3.73 kcal/g) for 6 weeks. Because WD and chow fed rats consume different amounts of calories per day during the first week, a WD-pair fed (WDpf) group was included as a control (n=12) to ensure that the observed effects were not due to greater energy intake. For the pair-feeding procedure, each WDpf animal was weight-paired with one Cal rat. The caloric intake of each Cal rats was measured daily. WDpf animals were given the quantity of diet calculated to equal the amount of calories ingested by their paired Cal. One third of the daily ration was given at 8am and the remaining two third at 8pm.Since this pair-feeding procedure alters the natural feeding pattern, we added a fourth group of rats (Cpf, n=6). These latter were fed a standard chow at the same caloric level than their weight-paired Cal rat and with the same feeding pattern than WDpf rats. Cpf and WDpf rats were pair-fed during the first week exclusively and fed *ad libitum* with their respective diets for 5 weeks. Body weight and food intake were measured daily the first week and twice a week for the remaining dietary intervention.

Serum and tissue collection

After 6 weeks on respective diets and after an overnight fast and 2-hr refeed, rats were euthanized by cardiac puncture under deep anesthesia induced by CO_2 asphyxia. Blood was collected by cardiac puncture and serum was obtained after centrifugation (4°C; 10 000 RPM, 15 min) and frozen at -80°C.

Fat pads (mesenteric, epididymal and retroperitoneal) weight was measured and adiposity was calculated as the sum of fat pad weights / body weight * 100. Luminal contents, tissue sections and mucosa scrapping from ileum and caecum were flash frozen in liquid nitrogen and stored at -80°C. Segments of ileum and caecum were collected and stored in cold DMEM (Thermofisher Scientific, Waltham, MA USA) for Ussing chambers measurements. Liver were flash frozen in liquid nitrogen and stored at -80°C. For histological measurement, sections of mesenteric fat, liver, ileum and colon were fixed in 4% formaldehyde for 24h and stored in 70% ethanol for further analysis.

Ex vivo permeability

Intestinal tissues were opened along the mesenteric border and mounted in Ussing chamber (Physiologic Instrument, San Diego, USA). The chamber opening exposed 0.5 cm^2 of tissue surface area to 2.5 mL of circulating oxygenated Krebs-glucose (10mM) and Krebs-mannitol (10mM) buffers at 37°C on the serosal and luminal sides, respectively. Tissues were short-circuited and Conductance (G) was determined at baseline as an indicator of paracellular ion flux and expressed as $mS.cm^2$. The transcellular and LPS permeabilities were determined as the flux of horseradish peroxidase (HRP Type II, Sigma-Aldrich, Saint-Quentin Fallavier, France) and FITC-LPS (Lipopolysaccharide from Escherichia coli 0111:B4, Sigma-Aldrich), respectively. FITC-LPS (40µg/ml) and HRP (200µg/ml) were added into the mucosal chamber at t0. Two hundred microliters samples were collected at 30-min intervals during 120 minutes from the serosal chambers and replaced with Krebs-glucose to maintain a constant volume within chambers. Concentration of FITC-LPS was measured by fluorimetry (fluorimeter LB940 Mithras; Berthold Technologies, Thoiry, France), whereas concentration of HRP was determined using spectrophotometry (Multiskan spectrum; Thermo Labsystem, Midland, Canada) after enzymatic reaction using o-dianisidine as substrate (Sigma-Aldrich). Mucosal-to serosal fluxes were then calculated and expressed as nanograms per square centimeter per hour.

Serum analyses

Lipopolysaccharide-binding protein levels were measured in serum samples via ELISA kit according to manufacturer's recommendations (Biometec, Greifswald, Germany). Serum aspartate

aminotransferase activity (ASAT) and alanine aminotransferase activity (ALAT) measurements were performed on a Roche/Hitachi system using adapted kits (Cobas analyzer, Roche Diagnostic, Meylan, France) and kindly performed by Dr Nicolas Collet from Pontchaillou Rennes CHU, Biochemistry Laboratory.

Serum endotoxemia was determined using the LAL assay in kinetic chromogenic conditions (Associate of Cape Cod) as previously described (44).

Histology

Mesenteric fat samples and liver were embedded in paraffin and cut in 10µm and 3µm sections respectively. Sections were then stained with hematoxylin and eosin. Mesenteric fat sections were examined under a light microscope (Nikon DS-Ri2) and images were taken at 100x magnification using NIS-Elements software. The area of adipocytes was measured with ImageJ 1.50i digital imaging processing software. Images from liver sections were randomly taken at 20x magnification under a light microscope (Nikon DS-Ri2). Image analysis using dedicated software (NIS-Elements AR3.0 software, Nikon Instruments) was performed to automatically detect lipid droplets and quantify their surface.

Ileum and colon samples were embedded in paraffin and cut in 5-µm sections. Both sections were then stained with periodic acid-Schiff-alcian blue (PAS/AB) and examined under a light microscope (Nikon ECLIPSE E400; Nikon Instrument) equipped with image analysis software. Villi length, crypt depth and goblet cell (GC) number were measured and counted in 20 well-oriented crypt-villus units. Presence of mucus in the lumen was scored visually from 0 to 2, 0 being no staining of mucus in the lumen and 2 large staining of mucus in the lumen. All the measurements were performed blinded for dietary group.

Triglycerides liver analysis

Liver lipids were extracted from 100 mg of liver tissue by the Folch method using chloroform and methanol. Triglycerides contents were then determined by colorimetric method according to manufacturer's recommendations (Triglyceride Quantification Assay Kit, Abcam, Cambridge, UK).

183

184 *Tissue RNA extraction and quantitative RT-PCR*

185 Total RNA from ileal, caecal and liver samples was extracted *via* the Trizol method (15596-018;
186 Thermofischer Scientific) and quantified using a spectrophotometer (Denovix, Wilmington, DE,
187 USA). 2µg RNA was converted to cDNA using a High Capacity Complementary DNA Reverse
188 Transcription Kit (Applied Biosystems, Foster City, CA, USA) following manufacturer's protocol.
189 Real-Time PCR was performed with the StepOnePlus real-time PCR machine using SyberGreen
190 master mix (Fischer Scientific) for detection. Primers for selected genes (Table 1) were designed using
191 Integrated DNA Technologies Primer Quest. HPRT-1, GAPDH and Actin were used as housekeeping
192 genes, using their mean Ct.

193

194 *Microbial DNA extraction and quantitative RT-PCR*

195 Total DNA was extracted from caecal luminal contents using the ZR Fecal DNA MiniPrep kit (Zymo
196 Research, Irvine, CA, USA). Then, DNA was quantified using a spectrophotometer (Denovix). Real-
197 Time PCR was performed with the StepOnePlus real-time PCR machine using SyberGreen master mix
198 for detection. Primers for selected 16S genes specific to each phylum are recapitulated in Table 1.
199 Universal 16S rRNA was used to normalize data.

200

201 *Statistical analysis*

202 Statistical analysis was performed on Graphpad Prism software (v5, San Diego, CA, USA) and data
203 are expressed as means ± SEM. Data were analyzed using two-ways ANOVA testing diet, feeding
204 pattern and diet X feeding pattern, with Bonferroni post hoc tests. For body weight and food intake
205 analysis, diet, feeding pattern, time, diet X feeding pattern effects were analyzed by ANOVA using R
206 software. $P<0.05$ was considered significant. Correlation analysis between data was performed using
207 Graphpad Prism.

208

209

Results

Six weeks WD feeding results in mild obese phenotype, irrespective of initial caloric intake

WDal rats had a greater energy intake during the first week of the dietary intervention (Fig 1A) while, as designed, WDpf rats had comparable energy intake than Cal rats thus avoiding the WD-induced first week hyperphagia (Fig 1A). From week 2 to 6, C animals ate slightly more calories than WD rats (diet effect P=0.049, Fig 1B).

Western diet-fed rats exhibited greater weight gain (diet P=0.004) compared to C rats, irrespective of the first week energy intake (Fig 1C). They exhibited marked adiposity with a 1.5-fold greater adiposity index compared to C animals, irrespective of initial food intake (diet P<0.0001, Fig 1D). This enhanced adiposity was due to elevated mesenteric, retroperitoneal and epididymal fat pad weights (data not shown). Six weeks of WD increased mesenteric fat adipocyte average surface (diet P = 0.011, Fig 1D).

Hepatic steatosis was evaluated by quantification of lipid droplet surface on histological slides and quantification of liver triglyceride content. Serum levels of ALAT and ASAT were used to evaluate hepatic function. WD rats exhibited increased presence of lipid droplets, mainly macro-vesicular as observed visually (P=0.039, Fig 1F). This was confirmed in WD rats by greater liver triglycerides content than C rats (diet P <0.0001, Fig 1G). ASAT serum levels were increased in WD-fed rats (diet P=0.022, Fig 1H). ALAT concentrations were not influenced by diet (Fig 1I).

DIO is characterized by chronic low grade inflammation likely originating from the intestine and spreading to other tissues (20). Therefore, we measured mRNA levels of the pro-inflammatory cytokine IL1-β in the ileum, caecum and liver. Six-week WD consumption significantly increased *il-1β* mRNA level in the caecum, but not in the ileum (Table 2). Hepatic *il-1β* mRNA levels were not different between WD and C fed rats.

Six weeks WD feeding induces metabolic endotoxemia

Endotoxemia evaluated by serum LPS was not significantly different between dietary groups (Fig 2A). Yet, WDpf animals displayed high heterogeneity in serum LPS with values ranging from 0.02 to 25.85

EU/mL.We measured serum LBP concentration, the main LPS circulating transporter considered as marker of hepatic exposure to LPS and thus metabolic endotoxemia. WD-fed rats exhibited a 3.3-fold increase (diet P=0.003, Fig 2B) in LBP serum concentration relative to C rats, irrespective of initial energy intake. This increased exposure of the liver to LPS was confirmed by greater hepatic *lbp* mRNA level in WD-fed animals compared to C rats (diet, P=0.006, Fig 2C) and significant correlation between *lbp* mRNA level and serum LBP concentration (r=0.742 and P<0.0001, Fig 2D).

Six week WD feeding modifies microbiota composition

Obesity is associated with alteration in intestinal bacterial composition that might result in increased LPS-bearing Gram negative bacteria abundance in the lumen. We therefore seek to evaluate the level of the major phyla present in the caecum. Levels of Bacteroidetes (Fig 3A), Firmicutes (Fig 3B) and Proteobacteria (Fig 3C) in caecal content were not altered by 6-week WD consumption, irrespective of the initial energy intake. However, WD fed rat exhibited significantly greater Verrucomicrobia levels in the caecum (+237%, diet P=0.004, Fig 3D), irrespective of the initial energy intake. Due to technical problems, we were not able to amplify Actinobacteria phylum and we used the genus *Bifidobacterium* as a representative of this phylum. *Bifidobacteria* levels were increased by 760% in WD animals (diet P=0.001, Fig 3E), irrespective of the initial energy intake.

Six week WF feeding profoundly affects ileal barrier function

Mucus secreted by GC is the first line of defense of the intestinal mucosa, limiting the presence of noxious molecules such as LPS on the apical side of epithelial cells. We therefore evaluated the number of GC in ileal and large intestinal mucosa using PAS/AB staining that colors mucins. In the ileum, the number of GC per villus or per crypt was reduced in WD rats (diet P<0.001, Fig 4A-B) with a tendency for a more pronounced reduction in WDpf rats (WDal vs WDpf P=0.07 in villi and P=0.056 in crypts). Since villi length, but not crypt depth, was decreased in WD-fed rats, irrespective of initial energy intake (data not shown), we calculated a number of GC / µm of villus or crypt to ensure that the reduction in GC number observed was not due to reduced villi size. In both villi and

crypts, the number of GC/µm was reduced by WD feeding (diet P<0.001, Fig 4C-D), with more pronounced effect in WDpf rats (Fig 4C-D).

PAS/AB staining also revealed large quantity of mucus in the ileal lumen of WD-fed rats (Fig 4E) that was quantified by scoring the presence (highest score) or absence (lowest score) of this luminal mucus. WD-fed rats exhibited a significantly greater score (diet *P*<0.0001, Fig 4F) than C rats, indicative of large amount of unorganized mucus in the lumen. WDpf rats had an even greater presence of mucus in the lumen compared to WDal (Fig 4F).

In the large intestine, no significant difference in colonic number of GC was observed between WD and C fed animals (data not shown). No mucus secretion in the lumen was noticed.

IAP is a brush border enzyme that dephosphorylates LPS, thus limiting its endotoxin activity. Ingestion of WD diet, irrespective of initial hyperphagia, dramatically increased IAP activity in both ileum and caecum (diet effect *P*=0.008 and *P*<0.0001, respectively, Table 3).

Ileal mucosa is also endowed with anti-microbial peptides (AMPs) secreted mainly by Paneth cells into the lumen, including regenerating family member (Reg)3-β specifically targeting Gram-negative bacteria (70). WD-fed rats exhibited a 3.3-fold decrease in ileal *reg3-β* expression after 6 weeks of diet compared to C rats (diet *P*=0.009, Table 3). We also measured the ileal gene expression of non-LPS specific AMPs: Reg3-γ, defensin 1 (DEFA-1), lysozyme C (LYZC) and group IIA phospholipase A2 (PLA2). Similarly to *reg3-β, reg3-γ* mRNA level was decreased in WD-fed rats relative to C rats (diet effect *P*=0.003). On the opposite, *lyzc, defa-1* and *pla-2* gene expressions were not influenced by the diet (Table 3). .

Intestinal passage of LPS was evaluated *ex vivo* in both ileum and caecum using Ussing chambers. Irrespective of initial energy intake, WD consumption induced a 1.5-fold increase in ileal LPS flux in WD-fed rats compared to C rats (diet *P*=0.027, Fig 5A). LPS flux across the caecum of WDal rats was not different from that of C rats (Fig 5B). However, WDpf rats exhibited a 2.2-fold increase in caecal LPS flux compared to WDal rats (Fig 5B). Paracellular and transcellular permeability measured by conductance and HRP flux, respectively, were also increased in the ileum of WD rats compared to C

ones, irrespective of the initial energy intake (diet P=0.04 and diet P=0.02, respectively, Fig 5 C-E). No differences were observed in caecal paracellular and transcellular permeability between WD and C animals (Fig 5 D-F)

Intestinal barrier function was also assessed by measuring the gene expression of several tight junction proteins (ZO-1, Claudin-1 and-2, occludin) and of MLCK, involved in myosin light chain phosphorylation and tight junction opening. *Occludin* mRNA level was 1.5-fold lower (diet P=0.003, Table 4) and that of *claudin-2* tended to be also lower (diet, P=0.07, Table 4) in the caecum of WD rats compared to C ones. Diet did not impact the expression of the other tight junction proteins and MLCK in the caecum or in the ileum (Table 3).

Hepatic LPS detoxification protein and enzymes

Hepatic gene expression of the two majors enzymes involved in liver LPS detoxification, AOAH and ALPL, was not influenced by diet, nor was that of SCARB-1, a scavenger receptor involved in LPS endocytosis from circulation into Kupffer cells (Table 5).

Ileal barrier function parameters correlate with metabolic endotoxemia

We next sought to investigate if ileal, caecal or hepatic parameters could explain LPS or LBP serum concentrations by correlating these different parameters. Serum LPS concentration correlated positively with ileal permeability parameters, including LPS and HRP fluxes across the ileum (P=0.003, Fig 6A-B and 0.013, Fig 6A respectively) but also ileal IAP activity (P=0.018, Fig6 A&C), Proteobacteria level (P=0.013, Fig 6A&D) and hepatic *aoah* mRNA levels (P=0.007, Fig 6A&E). Serum LBP concentration correlated positively with ileal barrier function parameters (LPS and HRP flux across ileal mucosa, P=0.0001, Fig6 A&F and 0.003, Fig6A, respectively and ileal conductance, P=0.004, Fig 6A, mucus secretion score in ileal lumen, P=0.01, Fig6 A&G), ileal and caecal IAP activity (P<0.0001 Fig 6A&H and 0.03, Fig 6A, respectively), Verrucomicrobia level (P=0.037, Fig 6 A&I) and negatively with ileal GC number in villi and crypts (P=0.01, Fig 6A&J and 0.025, Fig 6A, respectively) and Firmicutes level (P=0.025, Fig 6A&K).

Discussion

Despite the numerous intestinal and hepatic mechanisms limiting the entry and dissemination of gut-derived LPS into the systemic circulation, low, yet significant, amounts of LPS are found in the plasma of obese people, leading to low grade inflammation. We hypothesized that one or several of these mechanisms are impaired during DIO, resulting in elevated endotoxemia. In our model of mild obesity induced by 6 weeks of WD feeding, we observed disrupted ileal gut barrier function as demonstrated by reduced AMPs level, increased ileal IAP activity, altered mucus secretion and increased LPS flux across the ileum. The caecum barrier function was less altered, except in WDpf rats which exhibited increased passage of LPS. We also observed alteration of the gut microbiota with WD feeding but hepatic detoxification mechanisms were poorly affected at this stage of obesity. Correlation of all these data highlighted ileal defects as key drivers of metabolic endotoxemia.

Western-diet feeding in our model resulted in a mild obesity phenotype with greater weight gain, adiposity and enlargement of adipocytes compared to C rats but few metabolic consequences since the liver was only slightly affected by the diet. Indeed, we observed increased accumulation of triglycerides and of lipid droplets in the liver without reaching the level of steatosis defined as >5% of liver tissue section. We also observed a slight increase (+25%) in serum ASAT but not in ALAT and no signs of hepatic inflammation as documented by similar IL-1β gene expression in C and WD rats. Altogether, this suggests only few hepatic disturbances at this stage of obesity. On the other hand, caecal *il-1β* mRNA level was increased in WD rats. High-fat diet-induced intestinal inflammation precedes and correlates with later obesity and insulin resistance in mice (20). This reinforces the fact that our model is a mild obesity model with only initial intestinal inflammation that has not spread to the rest of the body yet.

Serum LPS concentration was not significantly increased in our WD-fed animals. However, they exhibited hepatic LPS exposure as demonstrated by increased hepatic *lbp* mRNA levels and serum LBP concentrations. LBP is an acute-phase protein synthesized in the liver in response to LPS (36). Considering that LPS has a short half-life and that LBP represents the innate immune response

triggered by LPS, serum LBP concentration is an indirect way to evaluate circulating LPS and is now considered as a good marker of metabolic endotoxemia (5, 27, 41, 73). The reason why we were not able to observe increased serum LPS in WD-fed rats is unknown but might be related to the stage of mild obesity of our rats whereby the multiple factors usually neutralizing LPS are not yet overwhelmed by chronic exposure to LPS and still able to efficiently detoxify LPS.

Because WD feeding in rodent is associated with caloric overconsumption during the first days of diet consumption (27, 77, 78), we included a group of pair-fed rats fed the WD without the initial hyperphagia, thus avoiding confounding factors. Previous studies reported that reducing WD calories intake attenuated but did not prevent the development of obesity and associated metabolic disorders (18, 58, 77, 78). Similarly, we demonstrated that weight gain, increased adiposity and hepatic parameters at week 6 were not dependent on initial energy intake. Despite the absence of significant difference in serum LPS between WD and C-fed rats it is noteworthy that the WDpf group presented a large variability in serum LPS levels. In rodents, it is usual to observe variability in response to WD feeding (46, 79). Elucidating why some of these animals exhibited such variability was beyond the scope of this study. Yet we noticed that WDpf rats exhibited elevated LPS flux across the caecum, in addition to the increased ileal LPS flux and a more pronounced alteration GC and mucus physiology. The early hyperphagia seen in WD fed rats when they are switched from chow to WD is probably due to the increased palatability of the diet (69, 77). Recently, it was demonstrated that this early phase of hyperphagia is characterized by transient hepatic steatosis, inflammation and glucose intolerance that resolve before a second phase of metabolic disorders appears after prolonged WD consumption (45, 76, 77). Unlike in the adipose tissue or the liver, one-week WD *ad libitum* consumption does not trigger intestinal damages or inflammation in the ileum or caecum of rodents (27, 31). On the contrary, eosinophil depletion has even been observed during the first few days of high-fat diet consumption in mice (31). Our WDpf rats exhibited increased caecal *il-1β* mRNA compared to WDal and C rats at 1 week (personal communication), suggesting that hyperphagia is necessary to maintain gut homeostasis on the short term and that the natural early hyperphagia triggers signals that limit inflammation and gut barrier dysfunction also on the long-term. Yet, further research is needed to understand this early priming effect.

Anti-microbial peptides and mucosal enzymes, secreted by Paneth cells and enterocytes protect against microbial attachment and invasion and participate to the regulation of the gut barrier function(8, 62). Enterocytes also secrete IAP, a gut mucosal protein that detoxifies LPS which is then unable to trigger TLR-induced inflammation (39). There is conflicting evidence regarding how the intestine adapts its mucosal defense i.e. AMPs secretion and IAP activity, to WD feeding. We showed that 6-week WD feeding led to the reduction of Reg-3β and γ ileal gene expression, yet, upregulated ileal and caecal IAP activities. Although DIO-induced reduction in AMPs secretion is widely accepted in the literature (19, 22, 23), the beneficial purpose of this decreased bacterial degradation capacity remains unclear since Reg3-γ deficient mice exhibit elevated inflammatory responses to commensal and enteric pathogen (47). Moreover, Reg3-γ promotes bacterial segregation (68); hence the decreased AMPs expression might lead to increased proportion of Gram-negative bacteria close to the enterocytes. On the other hand, the increased IAP activity in DIO which has also already been described (49, 64, 80) is probably intended to reduce toxic LPS activity within the gut wall. The beneficial effect of IAP on WD-induced endotoxemia has been revealed using mice deficient for IAP that exhibited greater endotoxemia and obesity compared to wild type animals after WD feeding (33). However, this upregulation might be specific to dietary intervention duration or intestinal section since opposite results have also been described with either longer or shorter duration of WD consumption (17, 30). Interestingly, increased IAP activity in the ileum and to a lesser extent in the caecum was one of the main factors correlating positively with serum LPS and LBP. This positive correlation seems counter-intuitive as greater IAP activity should result in lower level of LPS in the mucosa, thus lower levels of serum LPS and LBP. However, it has been shown using a germ-free zebrafish model that bacterial LPS induce epithelial IAP gene expression and enzymatic activity in a MyD88-dependant manner (3). We can therefore hypothesize that the increased IAP activity in our model results from increased LPS luminal concentration, in line with increased LPS or LBP serum concentrations.

Changes in the gut barrier function have been described in several animal models of obesity (13, 17, 31, 66) and humans (26, 54, 72), yet with some discrepancies (55) and has been suggested to be one

403 of the cause of elevated endotoxemia. The controlled passage of antigen by the epithelium involves
404 two routes across enterocytes and/or colonocytes depending on the size and charge of antigen.
405 Paracellular permeability refers to the passage of small diameter molecules between adjacent intestinal
406 epithelial cells. This pathway is regulated by junctional complexes including tight junction proteins.
407 Transcellular route refers to the passage of larger molecules via endocytose. DIO has been associated
408 with increased paracellular permeability, along with decreased tight junction protein expression in
409 both humans and animals models (11, 13, 31). Although literature data are scarce, transcellular
410 permeability seems to be similarly increased in response to obesity or WD feeding (27). In our model,
411 paracellular and transcellular permeabilities, evaluated respectively by electric conductance and HRP
412 flux across the mucosa in Ussing chambers were increased in the ileum, but not the caecum of WD-fed
413 rats. Tight junction protein mRNA levels were poorly affected by the diet in both intestinal sections,
414 except for occludin and to a lesser extent claudin-2 mRNA levels in the caecum. It is noteworthy that a
415 direct link between tight junction protein mRNA levels and epithelial permeability cannot be drawn as
416 many factors regulate epithelial permeability, such as expression, localization and phosphorylation of
417 the different tight junction proteins within the cells (9).
418 To our knowledge, our study is the first to evaluate the passage of LPS across the intestinal mucosa
419 using Ussing chambers in an obesity model. LPS flux across the ileum strongly correlated with serum
420 LBP and to a lesser extent serum LPS. Similarly, in a model of pig divergent for food intake and
421 exhibiting differences in serum endotoxemia, Mani et al observed a positive correlation between
422 serum endotoxin concentrations and passage of LPS across ileal, but not colonic, mucosa mounted in
423 Ussing chamber (51). This reinforces the fact that LPS permeability specifically in the ileum could be
424 a key driver of metabolic endotoxemia. The precise mechanisms by which LPS crosses the intestinal
425 epithelium and possible regional variations along the gut remain unknown. According to its size (59),
426 LPS likely crosses IEC through a transcellular pathway rather than a paracellular route. In the small
427 intestine, LPS crosses the enterocytes together with lipid absorption through the chylomicrons
428 pathway in postprandial phases. In a fasted state, it has been suggested that LPS could cross the
429 intestinal epithelium either through enterocytes (4, 50) or mucus emptied-goblets cells (29) via the
430 recently described goblet-cell associated passage (GAP) (38). In our study, we observed a large

quantity of mucus in the lumen of WD-fed rats that could result from reduced degradation of mucus and/or recent mucus secretion just before euthanasia. We suggest that this increased presence of mucus within the ileal lumen is due to mucus secretion. Indeed, mucus secretion would result in emptying GC that would not be stained by the PAS/AB staining, in agreement with the reduced number of PAS/AB-stained GC also observed. This possibility is also strengthened by the fact that the number of PAS/AB-stained GC was negatively correlated with luminal mucus presence score ($r=-0.770$ and -0.733 for villi and crypt, respectively, $P<0.0001$ for both), suggesting a direct inverse relationship between this two phenomena. Moreover, this type of images has already been observed in mice intestine where mucus secretion from GC was induced by leptin (60). Leptinemia is probably increased in our WD-fed animals exhibiting an increased adiposity index compared to C rats and as already demonstrated in the same animal model (27). We therefore speculate that increased ileal mucus secretion and subsequent increased in empty GC might allow LPS crossing through GAP, resulting in elevated LPS flux as observed in Ussing chambers. However, we also observed increased in ileal HRP flux in WD animals suggesting that LPS might also cross the enterocytes through regular transcytosis pathway. Further research is therefore needed to determine which of these mechanisms is the main LPS route of passage in the ileum.

DIO has been associated with drastic changes in the composition of the gut microbiota (24). Yet the impact of such changes in intestinal ecology in term of luminal LPS concentration is difficult to interpret. Indeed, inconsistent results are found in literature concerning how WD consumption impacts quantity of luminal LPS. Whereas two studies showed increased quantity of fecal LPS in WD-fed mice (35, 40) suggesting an increase in Gram-negative bacteria proportion in the gut lumen, Everard et al showed by metagenomics, a decrease in the abundance of genes involved in LPS biosynthesis within the caecal lumen (23). By evaluating the levels of the main phyla in the caecum, we sought to estimate the Gram negative/positive ratio after 6 weeks of WD feeding. We observed increased levels of the phylum Verrucomicrobia and of the genus *Bifidobacterium* (representative of Actinobacteria) in WD-fed rats. In healthy rats, Verrucomicrobia account for 2% of the caecal microbiota and Actinobacteria for less than 0.1% (27). Hence, the elevation in the Gram-positive Bifidobacterium

459 level is probably irrelevant compared to the increase in the Gram-negative Verrucomicrobia in terms
460 of Gram+/Gram- ratio. However, considering the small proportion of Verrucomicrobia (2%) compared
461 to Firmicutes and Bacteroidetes that represent more than 90% of bacteria harboring the colon, the
462 increased Gram-negative bacteria observed might also be poorly relevant in term of LPS luminal
463 concentration. Interestingly, our correlation analysis highlighted correlations between serum LPS
464 and/or LBP and the Gram-negative phyla Proteobacteria and Verrucomicrobia (positive correlations)
465 and negative correlation with the gram positive Firmicutes. Thus the Garm-positive / Gram-negative
466 composition and balance within the gut appears to also be a key driver of metabolic endotoxemia.
467
468 The liver is the main internal organ involved in LPS detoxification and disposal processes. Within
469 hepatocytes, LPS is endocytosed by Scavenger-Receptor (71) and detoxified by two majors enzymes:
470 AOAH (65) and ALPL (2). Those two enzymes are both upregulated in sepsis, characterized by high
471 concentration of LPS (57, 67). Our study is the first to investigate the impact of DIO on LPS liver
472 detoxification enzyme expression. Consumption of WD for 6 weeks did not significantly modify
473 hepatic gene expressions of AOAH and ALPL despite hepatic LPS exposure as demonstrated by
474 increased *lbp* mRNA and plasma LBP. This suggests either a dose effect, whereby a certain amount of
475 LPS is needed to induce detoxification enzyme up-regulation or a location effect as gut-derived LPS in
476 our model travels through the portal vein, thus achieving high intra-sinusoidal LPS concentrations as
477 opposed to experimental model of sepsis were LPS is injected intravenously. However, despite
478 absence of significant increase in AOAH gene expression, a significant correlation between serum
479 LPS and AOAH gene expression was observed. AOAH is an important lipase enzyme that selectively
480 removes the secondary fatty acyl chains attached to the primary chains in the lipid A moiety and
481 detoxifies endotoxin (65). It has been shown in immune cells that its expression is up-regulated by
482 LPS exposure (15) . Increased hepatic exposure to LPS either through an increased passage across the
483 ileum or through the blood circulation could therefore up-regulates hepatic AOAH gene expression.
484
485 In conclusion, our data demonstrate that 6-week WD feeding in rats leads to multiple adaptations of
486 the intestinal mechanisms involved in protection against LPS entry and dissemination within the host.

They also highlight that the disrupted ileal barrier function characterized by impairment of mucosa defense mechanisms associated to increased ileal permeability to LPS and probably to an unbalance in the Gram-negative / Gram positive ratio within the gut microbiota is central to the development of metabolic endotoxemia. Therefore, the ileum should be chosen as a target organ for developing efficient strategies to reduce/decrease/blunt metabolic endotoxemia. Another novelty of our study is that by using a pair-feeding procedure we highlighted the fact that the first week hyperphagia under high fat diet might play a role in maintaining long term caecal homeostasis. One limitation of our study is that we did not investigate the mechanisms behind this effect, yet we used this variability to investigate more deeply gut-induced metabolic endotoxemia. Further studies are needed to understand the WDpf phenotype.

Acknowledgments

The authors are grateful to Dr. Kristina Hamilton for technical assistance in Ussing chamber experiments and rats handling. We acknowledge Adelaïde Prevotel, Michèle Formal, Armelle Cahu, Gwenaëlle Randuineau, Sylvie Guérin and Paul Meurice for technical assistance in histological analysis. We thank Regis Janvier for technical assistance in rats handling. We thank Veronique Romé and Laurence Le Normand for their help on molecular biology data analysis and colorimetric assays.

Grants

M. Guerville was funded by an INRA-Region Bretagne Fellowship.

Disclosures

No conflicts of interest, financial or otherwise are declared by the author(s).

References

1. **Andres SF, Santoro MA, Mah AT, Keku JA, Bortvedt AE, Blue RE, and Lund PK**. Deletion of intestinal epithelial insulin receptor attenuates high-fat diet-induced elevations in cholesterol and stem, enteroendocrine, and Paneth cell mRNAs. *American journal of physiology Gastrointestinal and liver physiology* 308: G100-111, 2015.
2. **Angelakis E, Armougom F, Carriere F, Bachar D, Laugier R, Lagier JC, Robert C, Michelle C, Henrissat B, and Raoult D**. A Metagenomic Investigation of the Duodenal Microbiota Reveals Links with Obesity. *PloS one* 10: e0137784, 2015.
3. **Bates JM, Akerlund J, Mittge E, and Guillemin K**. Intestinal alkaline phosphatase detoxifies lipopolysaccharide and prevents inflammation in zebrafish in response to the gut microbiota. *Cell host & microbe* 2: 371-382, 2007.
4. **Beatty WL, Meresse S, Gounon P, Davoust J, Mounier J, Sansonetti PJ, and Gorvel JP**. Trafficking of Shigella lipopolysaccharide in polarized intestinal epithelial cells. *The Journal of cell biology* 145: 689-698, 1999.
5. **Benoit B, Laugerette F, Plaisancie P, Geloen A, Bodennec J, Estienne M, Pineau G, Bernalier-Donadille A, Vidal H, and Michalski MC**. Increasing fat content from 20 to 45 wt% in a complex diet induces lower endotoxemia in parallel with an increased number of intestinal goblet cells in mice. *Nutrition research* 35: 346-356, 2015.
6. **Benoit B, Plaisancie P, Geloen A, Estienne M, Debard C, Meugnier E, Loizon E, Daira P, Bodennec J, Cousin O, Vidal H, Laugerette F, and Michalski MC**. Pasture v. standard dairy cream in high-fat diet-fed mice: improved metabolic outcomes and stronger intestinal barrier. *The British journal of nutrition* 112: 520-535, 2014.
7. **Bevins CL, and Salzman NH**. Paneth cells, antimicrobial peptides and maintenance of intestinal homeostasis. *Nature reviews Microbiology* 9: 356-368, 2011.
8. **Bischoff SC, Barbara G, Buurman W, Ockhuizen T, Schulzke JD, Serino M, Tilg H, Watson A, and Wells JM**. Intestinal permeability--a new target for disease prevention and therapy. *BMC gastroenterology* 14: 189, 2014.
9. **Bischoff SC, Barbara G, Buurman W, Ockhuizen T, Schulzke JD, Serino M, Tilg H, Watson A, and Wells JM**. Intestinal permeability--a new target for disease prevention and therapy. *BMC gastroenterology* 14: 189, 2014.
10. **Boutagy NE, McMillan RP, Frisard MI, and Hulver MW**. Metabolic endotoxemia with obesity: Is it real and is it relevant? *Biochimie* 124: 11-20, 2016.
11. **Brun P, Castagliuolo I, Di Leo V, Buda A, Pinzani M, Palu G, and Martines D**. Increased intestinal permeability in obese mice: new evidence in the pathogenesis of nonalcoholic steatohepatitis. *American journal of physiology Gastrointestinal and liver physiology* 292: G518-525, 2007.
12. **Cani PD, Amar J, Iglesias MA, Poggi M, Knauf C, Bastelica D, Neyrinck AM, Fava F, Tuohy KM, Chabo C, Waget A, Delmee E, Cousin B, Sulpice T, Chamontin B, Ferrieres J, Tanti JF, Gibson GR, Casteilla L, Delzenne NM, Alessi MC, and Burcelin R**. Metabolic endotoxemia initiates obesity and insulin resistance. *Diabetes* 56: 1761-1772, 2007.
13. **Cani PD, Bibiloni R, Knauf C, Waget A, Neyrinck AM, Delzenne NM, and Burcelin R**. Changes in gut microbiota control metabolic endotoxemia-induced inflammation in high-fat diet-induced obesity and diabetes in mice. *Diabetes* 57: 1470-1481, 2008.
14. **Caroff M, and Karibian D**. Structure of bacterial lipopolysaccharides. *Carbohydrate research* 338: 2431-2447, 2003.
15. **Cody MJ**. Effect of inflammatory and anti-inflammatory stimuli on acyloxyacyl hydrolase gene expression and enzymatic activity in murine macrophages. *Journal of endotoxin research* 4: 371-379, 1997.

16. **Creely SJ, McTernan PG, Kusminski CM, Fisher f M, Da Silva NF, Khanolkar M, Evans M, Harte AL, and Kumar S**. Lipopolysaccharide activates an innate immune system response in human adipose tissue in obesity and type 2 diabetes. *American journal of physiology Endocrinology and metabolism* 292: E740-747, 2007.
17. **de La Serre CB, Ellis CL, Lee J, Hartman AL, Rutledge JC, and Raybould HE**. Propensity to high-fat diet-induced obesity in rats is associated with changes in the gut microbiota and gut inflammation. *American journal of physiology Gastrointestinal and liver physiology* 299: G440-448, 2010.
18. **de Meijer VE, Le HD, Meisel JA, Akhavan Sharif MR, Pan A, Nose V, and Puder M**. Dietary fat intake promotes the development of hepatic steatosis independently from excess caloric consumption in a murine model. *Metabolism: clinical and experimental* 59: 1092-1105, 2010.
19. **de Wit NJ, Bosch-Vermeulen H, de Groot PJ, Hooiveld GJ, Bromhaar MM, Jansen J, Muller M, and van der Meer R**. The role of the small intestine in the development of dietary fat-induced obesity and insulin resistance in C57BL/6J mice. *BMC medical genomics* 1: 14, 2008.
20. **Ding S, Chi MM, Scull BP, Rigby R, Schwerbrock NM, Magness S, Jobin C, and Lund PK**. High-fat diet: bacteria interactions promote intestinal inflammation which precedes and correlates with obesity and insulin resistance in mouse. *PloS one* 5: e12191, 2010.
21. **Erridge C, Bennett-Guerrero E, and Poxton IR**. Structure and function of lipopolysaccharides. *Microbes and infection / Institut Pasteur* 4: 837-851, 2002.
22. **Everard A, Geurts L, Caesar R, Van Hul M, Matamoros S, Duparc T, Denis RG, Cochez P, Pierard F, Castel J, Bindels LB, Plovier H, Robine S, Muccioli GG, Renauld JC, Dumoutier L, Delzenne NM, Luquet S, Backhed F, and Cani PD**. Intestinal epithelial MyD88 is a sensor switching host metabolism towards obesity according to nutritional status. *Nature communications* 5: 5648, 2014.
23. **Everard A, Lazarevic V, Gaia N, Johansson M, Stahlman M, Backhed F, Delzenne NM, Schrenzel J, Francois P, and Cani PD**. Microbiome of prebiotic-treated mice reveals novel targets involved in host response during obesity. *The ISME journal* 8: 2116-2130, 2014.
24. **Gerard P**. Gut microbiota and obesity. *Cellular and molecular life sciences : CMLS* 73: 147-162, 2016.
25. **Guerville M, and Boudry G**. Gastro-intestinal and hepatic mechanisms limiting the entry and dissemination of lipopolysaccharide into the systemic circulation. *American journal of physiology Gastrointestinal and liver physiology* ajpgi 00098 02016, 2016.
26. **Gummesson A, Carlsson LM, Storlien LH, Backhed F, Lundin P, Lofgren L, Stenlof K, Lam YY, Fagerberg B, and Carlsson B**. Intestinal permeability is associated with visceral adiposity in healthy women. *Obesity* 19: 2280-2282, 2011.
27. **Hamilton MK, Boudry G, Lemay DG, and Raybould HE**. Changes in intestinal barrier function and gut microbiota in high-fat diet-fed rats are dynamic and region dependent. *American journal of physiology Gastrointestinal and liver physiology* 308: G840-851, 2015.
28. **Hotamisligil GS**. Inflammation and metabolic disorders. *Nature* 444: 860-867, 2006.
29. **Howe SE, Lickteig DJ, Plunkett KN, Ryerse JS, and Konjufca V**. The uptake of soluble and particulate antigens by epithelial cells in the mouse small intestine. *PloS one* 9: e86656, 2014.
30. **Jiang T, Gao X, Wu C, Tian F, Lei Q, Bi J, Xie B, Wang HY, Chen S, and Wang X**. Apple-Derived Pectin Modulates Gut Microbiota, Improves Gut Barrier Function, and Attenuates Metabolic Endotoxemia in Rats with Diet-Induced Obesity. *Nutrients* 8: 2016.
31. **Johnson AM, Costanzo A, Gareau MG, Armando AM, Quehenberger O, Jameson JM, and Olefsky JM**. High fat diet causes depletion of intestinal eosinophils associated with intestinal permeability. *PloS one* 10: e0122195, 2015.
32. **Johnson AR, Milner JJ, and Makowski L**. The inflammation highway: metabolism accelerates inflammatory traffic in obesity. *Immunological reviews* 249: 218-238, 2012.
33. **Kaliannan K, Hamarneh SR, Economopoulos KP, Nasrin Alam S, Moaven O, Patel P, Malo NS, Ray M, Abtahi SM, Muhammad N, Raychowdhury A, Teshager A, Mohamed MM, Moss AK, Ahmed R, Hakimian S, Narisawa S, Millan JL, Hohmann E, Warren HS, Bhan AK, Malo MS, and**

610 **Hodin RA**. Intestinal alkaline phosphatase prevents metabolic syndrome in mice. *Proceedings of the*
611 *National Academy of Sciences of the United States of America* 110: 7003-7008, 2013.
612 34. **Kallio KA, Hatonen KA, Lehto M, Salomaa V, Mannisto S, and Pussinen PJ**. Endotoxemia,
613 nutrition, and cardiometabolic disorders. *Acta diabetologica* 52: 395-404, 2015.
614 35. **Kim KA, Gu W, Lee IA, Joh EH, and Kim DH**. High fat diet-induced gut microbiota exacerbates
615 inflammation and obesity in mice via the TLR4 signaling pathway. *PloS one* 7: e47713, 2012.
616 36. **Kirschning C, Unbehaun A, Lamping N, Pfeil D, Herrmann F, and Schumann RR**. Control of
617 transcriptional activation of the lipopolysaccharide binding protein (LBP) gene by proinflammatory
618 cytokines. *Cytokines, cellular & molecular therapy* 3: 59-62, 1997.
619 37. **Kless C, Muller VM, Schuppel VL, Lichtenegger M, Rychlik M, Daniel H, Klingenspor M, and**
620 **Haller D**. Diet-induced obesity causes metabolic impairment independent of alterations in gut barrier
621 integrity. *Molecular nutrition & food research* 59: 968-978, 2015.
622 38. **Knoop KA, McDonald KG, McCrate S, McDole JR, and Newberry RD**. Microbial sensing by
623 goblet cells controls immune surveillance of luminal antigens in the colon. *Mucosal immunology* 8:
624 198-210, 2015.
625 39. **Lalles JP**. Intestinal alkaline phosphatase: novel functions and protective effects. *Nutrition*
626 *reviews* 72: 82-94, 2014.
627 40. **Lau E, Marques C, Pestana D, Santoalha M, Carvalho D, Freitas P, and Calhau C**. The role of
628 I-FABP as a biomarker of intestinal barrier dysfunction driven by gut microbiota changes in obesity.
629 *Nutrition & metabolism* 13: 31, 2016.
630 41. **Laugerette F, Alligier M, Bastard JP, Drai J, Chanseaume E, Lambert-Porcheron S, Laville M,**
631 **Morio B, Vidal H, and Michalski MC**. Overfeeding increases postprandial endotoxemia in men:
632 Inflammatory outcome may depend on LPS transporters LBP and sCD14. *Mol Nutr Food Res* 58: 1513-
633 1518, 2014.
634 42. **Laugerette F, Alligier M, Bastard JP, Drai J, Chanseaume E, Lambert-Porcheron S, Laville M,**
635 **Morio B, Vidal H, and Michalski MC**. Overfeeding increases postprandial endotoxemia in men:
636 Inflammatory outcome may depend on LPS transporters LBP and sCD14. *Molecular nutrition & food*
637 *research* 58: 1513-1518, 2014.
638 43. **Laugerette F, Furet JP, Debard C, Daira P, Loizon E, Geloen A, Soulage CO, Simonet C, Lefils-**
639 **Lacourtablaise J, Bernoud-Hubac N, Bodennec J, Peretti N, Vidal H, and Michalski MC**. Oil
640 composition of high-fat diet affects metabolic inflammation differently in connection with endotoxin
641 receptors in mice. *American journal of physiology Endocrinology and metabolism* 302: E374-386,
642 2012.
643 44. **Laugerette F, Pineau G, Vors C, and Michalski M**. Endotoxemia Analysis by the Limulus
644 Amoebocyte Lysate Assay in Different Mammal Species Used in Metabolic Studies. *Journal of*
645 *Analytical & Bioanalytical Techniques* 6: 251, 2015.
646 45. **Lee YS, Li P, Huh JY, Hwang IJ, Lu M, Kim JI, Ham M, Talukdar S, Chen A, Lu WJ,**
647 **Bandyopadhyay GK, Schwendener R, Olefsky J, and Kim JB**. Inflammation is necessary for long-term
648 but not short-term high-fat diet-induced insulin resistance. *Diabetes* 60: 2474-2483, 2011.
649 46. **Leibowitz KL, Chang GQ, Pamy PS, Hill JO, Gayles EC, and Leibowitz SF**. Weight gain model in
650 prepubertal rats: prediction and phenotyping of obesity-prone animals at normal body weight.
651 *International journal of obesity* 31: 1210-1221, 2007.
652 47. **Loonen LM, Stolte EH, Jaklofsky MT, Meijerink M, Dekker J, van Baarlen P, and Wells JM**.
653 REG3gamma-deficient mice have altered mucus distribution and increased mucosal inflammatory
654 responses to the microbiota and enteric pathogens in the ileum. *Mucosal immunology* 7: 939-947,
655 2014.
656 48. **Luck H, Tsai S, Chung J, Clemente-Casares X, Ghazarian M, Revelo XS, Lei H, Luk CT, Shi SY,**
657 **Surendra A, Copeland JK, Ahn J, Prescott D, Rasmussen BA, Chng MH, Engleman EG, Girardin SE,**
658 **Lam TK, Croitoru K, Dunn S, Philpott DJ, Guttman DS, Woo M, Winer S, and Winer DA**. Regulation of
659 obesity-related insulin resistance with gut anti-inflammatory agents. *Cell metabolism* 21: 527-542,
660 2015.

49. **Lynes M, Narisawa S, Millan JL, and Widmaier EP**. Interactions between CD36 and global intestinal alkaline phosphatase in mouse small intestine and effects of high-fat diet. *American journal of physiology Regulatory, integrative and comparative physiology* 301: R1738-1747, 2011.
50. **Mani V, Hollis JH, and Gabler NK**. Dietary oil composition differentially modulates intestinal endotoxin transport and postprandial endotoxemia. *Nutrition & metabolism* 10: 6, 2013.
51. **Mani V, Hollis JH, and Gabler NK**. Dietary oil composition differentially modulates intestinal endotoxin transport and postprandial endotoxemia. *Nutrition & metabolism* 10: 6, 2013.
52. **Moreira AP, Texeira TF, Ferreira AB, Peluzio Mdo C, and Alfenas Rde C**. Influence of a high-fat diet on gut microbiota, intestinal permeability and metabolic endotoxaemia. *The British journal of nutrition* 108: 801-809, 2012.
53. **Moreno-Navarrete JM, Ortega FJ, Bassols J, Ricart W, and Fernandez-Real JM**. Decreased circulating lactoferrin in insulin resistance and altered glucose tolerance as a possible marker of neutrophil dysfunction in type 2 diabetes. *The Journal of clinical endocrinology and metabolism* 94: 4036-4044, 2009.
54. **Moreno-Navarrete JM, Sabater M, Ortega F, Ricart W, and Fernandez-Real JM**. Circulating zonulin, a marker of intestinal permeability, is increased in association with obesity-associated insulin resistance. *PloS one* 7: e37160, 2012.
55. **Muller VM, Zietek T, Rohm F, Fiamoncini J, Lagkouvardos I, Haller D, Clavel T, and Daniel H**. Gut barrier impairment by high-fat diet in mice depends on housing conditions. *Molecular nutrition & food research* 60: 897-908, 2016.
56. **Naito E, Yoshida Y, Makino K, Kounoshi Y, Kunihiro S, Takahashi R, Matsuzaki T, Miyazaki K, and Ishikawa F**. Beneficial effect of oral administration of Lactobacillus casei strain Shirota on insulin resistance in diet-induced obesity mice. *Journal of applied microbiology* 110: 650-657, 2011.
57. **Ojogun N, Kuang TY, Shao B, Greaves DR, Munford RS, and Varley AW**. Overproduction of acyloxyacyl hydrolase by macrophages and dendritic cells prevents prolonged reactions to bacterial lipopolysaccharide in vivo. *The Journal of infectious diseases* 200: 1685-1693, 2009.
58. **Petro AE, Cotter J, Cooper DA, Peters JC, Surwit SJ, and Surwit RS**. Fat, carbohydrate, and calories in the development of diabetes and obesity in the C57BL/6J mouse. *Metabolism: clinical and experimental* 53: 454-457, 2004.
59. **Petsch D, and Anspach FB**. Endotoxin removal from protein solutions. *Journal of biotechnology* 76: 97-119, 2000.
60. **Plaisancie P, Ducroc R, El Homsi M, Tsocas A, Guilmeau S, Zoghbi S, Thibaudeau O, and Bado A**. Luminal leptin activates mucin-secreting goblet cells in the large bowel. *American journal of physiology Gastrointestinal and liver physiology* 290: G805-812, 2006.
61. **Poltorak A, He X, Smirnova I, Liu MY, Van Huffel C, Du X, Birdwell D, Alejos E, Silva M, Galanos C, Freudenberg M, Ricciardi-Castagnoli P, Layton B, and Beutler B**. Defective LPS signaling in C3H/HeJ and C57BL/10ScCr mice: mutations in Tlr4 gene. *Science* 282: 2085-2088, 1998.
62. **Rodriguez-Pineiro AM, Bergstrom JH, Ermund A, Gustafsson JK, Schutte A, Johansson ME, and Hansson GC**. Studies of mucus in mouse stomach, small intestine, and colon. II. Gastrointestinal mucus proteome reveals Muc2 and Muc5ac accompanied by a set of core proteins. *American journal of physiology Gastrointestinal and liver physiology* 305: G348-356, 2013.
63. **Schumann RR, and Latz E**. Lipopolysaccharide-binding protein. *Chemical immunology* 74: 42-60, 2000.
64. **Sefcikova Z, Hajek T, Lenhardt L, Racek L, and Mozes S**. Different functional responsibility of the small intestine to high-fat/high-energy diet determined the expression of obesity-prone and obesity-resistant phenotypes in rats. *Physiological research / Academia Scientiarum Bohemoslovaca* 57: 467-474, 2008.
65. **Shao B, Lu M, Katz SC, Varley AW, Hardwick J, Rogers TE, Ojogun N, Rockey DC, Dematteo RP, and Munford RS**. A host lipase detoxifies bacterial lipopolysaccharides in the liver and spleen. *The Journal of biological chemistry* 282: 13726-13735, 2007.

66. **Suzuki T, and Hara H**. Dietary fat and bile juice, but not obesity, are responsible for the increase in small intestinal permeability induced through the suppression of tight junction protein expression in LETO and OLETF rats. *Nutrition & metabolism* 7: 19, 2010.
67. **Tuin A, Huizinga-Van der Vlag A, van Loenen-Weemaes AM, Meijer DK, and Poelstra K**. On the role and fate of LPS-dephosphorylating activity in the rat liver. *American journal of physiology Gastrointestinal and liver physiology* 290: G377-385, 2006.
68. **Vaishnava S, Yamamoto M, Severson KM, Ruhn KA, Yu X, Koren O, Ley R, Wakeland EK, and Hooper LV**. The antibacterial lectin RegIIIgamma promotes the spatial segregation of microbiota and host in the intestine. *Science* 334: 255-258, 2011.
69. **Valdivia S, Patrone A, Reynaldo M, and Perello M**. Acute high fat diet consumption activates the mesolimbic circuit and requires orexin signaling in a mouse model. *PloS one* 9: e87478, 2014.
70. **van Ampting MT, Loonen LM, Schonewille AJ, Konings I, Vink C, Iovanna J, Chamaillard M, Dekker J, van der Meer R, Wells JM, and Bovee-Oudenhoven IM**. Intestinally secreted C-type lectin Reg3b attenuates salmonellosis but not listeriosis in mice. *Infection and immunity* 80: 1115-1120, 2012.
71. **Van Bossuyt H, De Zanger RB, and Wisse E**. Cellular and subcellular distribution of injected lipopolysaccharide in rat liver and its inactivation by bile salts. *Journal of hepatology* 7: 325-337, 1988.
72. **Verdam FJ, Fuentes S, de Jonge C, Zoetendal EG, Erbil R, Greve JW, Buurman WA, de Vos WM, and Rensen SS**. Human intestinal microbiota composition is associated with local and systemic inflammation in obesity. *Obesity* 21: E607-615, 2013.
73. **Vors C, Pineau G, Drai J, Meugnier E, Pesenti S, Laville M, Laugerette F, Malpuech-Brugere C, Vidal H, and Michalski MC**. Postprandial Endotoxemia Linked With Chylomicrons and Lipopolysaccharides Handling in Obese Versus Lean Men: A Lipid Dose-Effect Trial. *The Journal of clinical endocrinology and metabolism* 100: 3427-3435, 2015.
74. **Waise TM, Toshinai K, Naznin F, NamKoong C, Md Moin AS, Sakoda H, and Nakazato M**. One-day high-fat diet induces inflammation in the nodose ganglion and hypothalamus of mice. *Biochemical and biophysical research communications* 464: 1157-1162, 2015.
75. **Wang J, Tang H, Zhang C, Zhao Y, Derrien M, Rocher E, van-Hylckama Vlieg JE, Strissel K, Zhao L, Obin M, and Shen J**. Modulation of gut microbiota during probiotic-mediated attenuation of metabolic syndrome in high fat diet-fed mice. *The ISME journal* 9: 1-15, 2015.
76. **Wiedemann MS, Wueest S, Item F, Schoenle EJ, and Konrad D**. Adipose tissue inflammation contributes to short-term high-fat diet-induced hepatic insulin resistance. *American journal of physiology Endocrinology and metabolism* 305: E388-395, 2013.
77. **Williams LM, Campbell FM, Drew JE, Koch C, Hoggard N, Rees WD, Kamolrat T, Thi Ngo H, Steffensen IL, Gray SR, and Tups A**. The development of diet-induced obesity and glucose intolerance in C57BL/6 mice on a high-fat diet consists of distinct phases. *PloS one* 9: e106159, 2014.
78. **Woods SC, Seeley RJ, Rushing PA, D'Alessio D, and Tso P**. A controlled high-fat diet induces an obese syndrome in rats. *The Journal of nutrition* 133: 1081-1087, 2003.
79. **Xia SF, Duan XM, Hao LY, Li LT, Cheng XR, Xie ZX, Qiao Y, Li LR, Tang X, Shi YH, and Le GW**. Role of thyroid hormone homeostasis in obesity-prone and obesity-resistant mice fed a high-fat diet. *Metabolism: clinical and experimental* 64: 566-579, 2015.
80. **Zhou X, Han D, Xu R, Li S, Wu H, Qu C, Wang F, Wang X, and Zhao Y**. A model of metabolic syndrome and related diseases with intestinal endotoxemia in rats fed a high fat and high sucrose diet. *PloS one* 9: e115148, 2014.

Figure legends

Figure 1: Western diet feeding induces a mild obesity phenotype

759 Daily average food intake on week 1 (A) and on the whole dietary intervention period (B), weight
760 gain over the 6-week period (C), adiposity index (D), mesenteric fat adipocyte average size (E),
761 hepatic steatosis (F), hepatic triglyceride content (G) and serum ASAT (H) and ALAT (I)
762 concentrations at week 6 for control *ad libitum* (Cal), control pair-fed (Cpf), WD *ad libitum* (WDal)
763 and WD pair-fed (WDpf) rats. Data are expressed as mean ± SEM. * P<0.05.

764 **Figure 2: Western diet feeding induces metabolic endotoxemia**

765 Serum concentration of LPS (A), LBP (B) and hepatic mRNA levels of *lbp* (C) of control *ad libitum*
766 (Cal), control pair-fed (Cpf), WD *ad libitum* (WDal) and WD pair-fed (WDpf) rats at week 6.
767 Correlation between hepatic *lbp* gene expression and serum LBP levels (D). Data are presented as
768 means ± SEM. * P<0.05.

769

770 **Figure 3: Western diet feeding alters caecal microbiota composition**

771 Levels of Bacteroidetes (A), Firmicutes (B), Proteobacteria (C), Verrucomicrobia (D) and
772 *Bifidobacteria* (E) in caecal content of control *ad libitum* (Cal), control pair-fed (Cpf), WD *ad libitum*
773 (WDal) and WD pair-fed (WDpf) rats at 6 weeks. (E). Data are presented as means ± SEM. * P<0.05.

774

775 **Figure 4: Western diet feeding reduces goblet cell number but increase luminal mucus in the**
776 **ileum**

777 Number of goblet cells (GC) per villus (A) or per crypt (B); number of GC / µm of villus (C) or crypt
778 (D) and score of presence of luminal mucus (F) in the ileum of control *ad libitum* (Cal), control pair-
779 fed (Cpf), WD *ad libitum* (WDal) and WD pair-fed (WDpf) rats at week 6. Representative histological
780 images of ileum sections stained with PAS/AB (I) of Cal, Cpf, WDal and WDpf rats at week 6 €. Data
781 are presented as means ± SEM. * P<0.05.

782

783 **Figure 5: Western diet feeding increases intestinal permeability**

784 LPS-FITC flux across ileum (A) and caecum (B), conductance of ileum (C) and caecum (D), HRP
785 flux across ileum (E) and caecum (F) of control *ad libitum* (Cal), control pair-fed (Cpf), WD *ad*

786 *libitum* (WDal) and WD pair-fed (WDpf) rats at week 6. Data are presented as means ± SEM.
787 *P<0.05.
788
789 **Figure 6: Correlation of serum LPS and LBP with intestinal and hepatic parameters**
790 Correlation matrix of serum LPS and LBP and intestinal and hepatic parameters involved in LPS
791 detoxification or disposal (A). Correlation of serum LPS with ileal LPS flux (B), ileal IAP activity (C),
792 Proteobacteria level (D) and hepatic aoah mRNA level (E). Correlation of serum LBP with ileal LPS
793 flux (F), score of mucus presence in the ileum (G), ileal IAP activity (H), Verrucomicrobioa level (I),
794 number of GC / µm in ileal villus (J) and Firmicutes level (K).

FIGURE 1

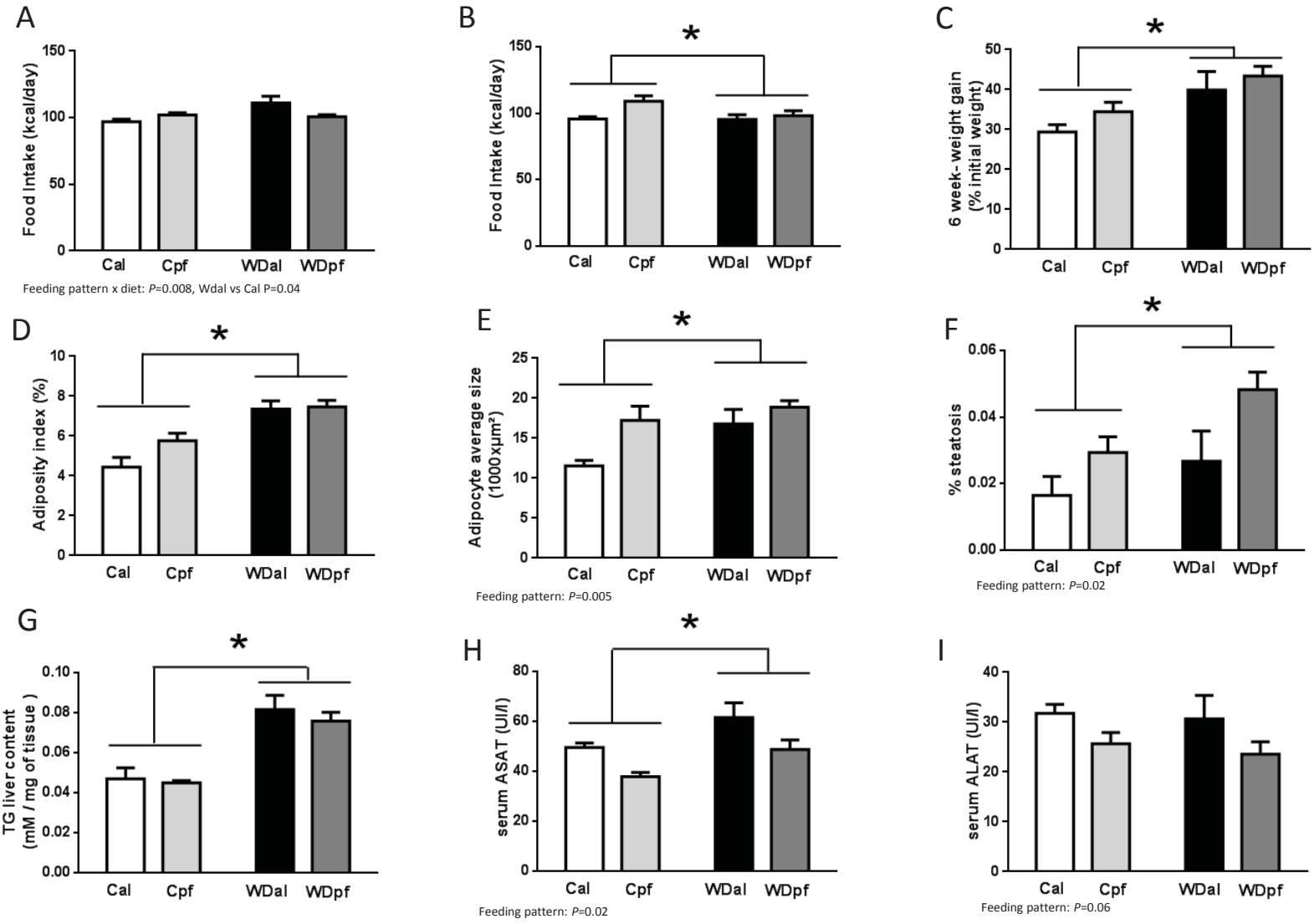
A
Food Intake (kcal/day)
150
100
50
0
Cal
Cpf
WDal
WDpf
Feeding pattern x diet: P=0.008, Wdal vs Cal P=0.04
B
*
Food Intake (kcal/day)
150
100
50
0
Cal
Cpf
WDal
WDpf
C
*
6 week- weight gain (% initial weight)
50
40
30
20
10
0
Cal
Cpf
WDal
WDpf
D
*
Adiposity index (%)
10
8
6
4
2
0
Cal
Cpf
WDal
WDpf
E
*
Adipocyte average size (1000xµm²)
25
20
15
10
5
0
Cal
Cpf
WDal
WDpf
Feeding pattern: P=0.005
F
*
% steatosis
0.06
0.04
0.02
0.00
Cal
Cpf
WDal
WDpf
Feeding pattern: P=0.02
G
*
TG liver content (mM / mg of tissue)
0.10
0.08
0.06
0.04
0.02
0.00
Cal
Cpf
WDal
WDpf
H
*
serum ASAT (UI/l)
80
60
40
20
0
Cal
Cpf
WDal
WDpf
Feeding pattern: P=0.02
I
serum ALAT (UI/l)
40
30
20
10
0
Cal
Cpf
WDal
WDpf
Feeding pattern: P=0.06

FIGURE 2

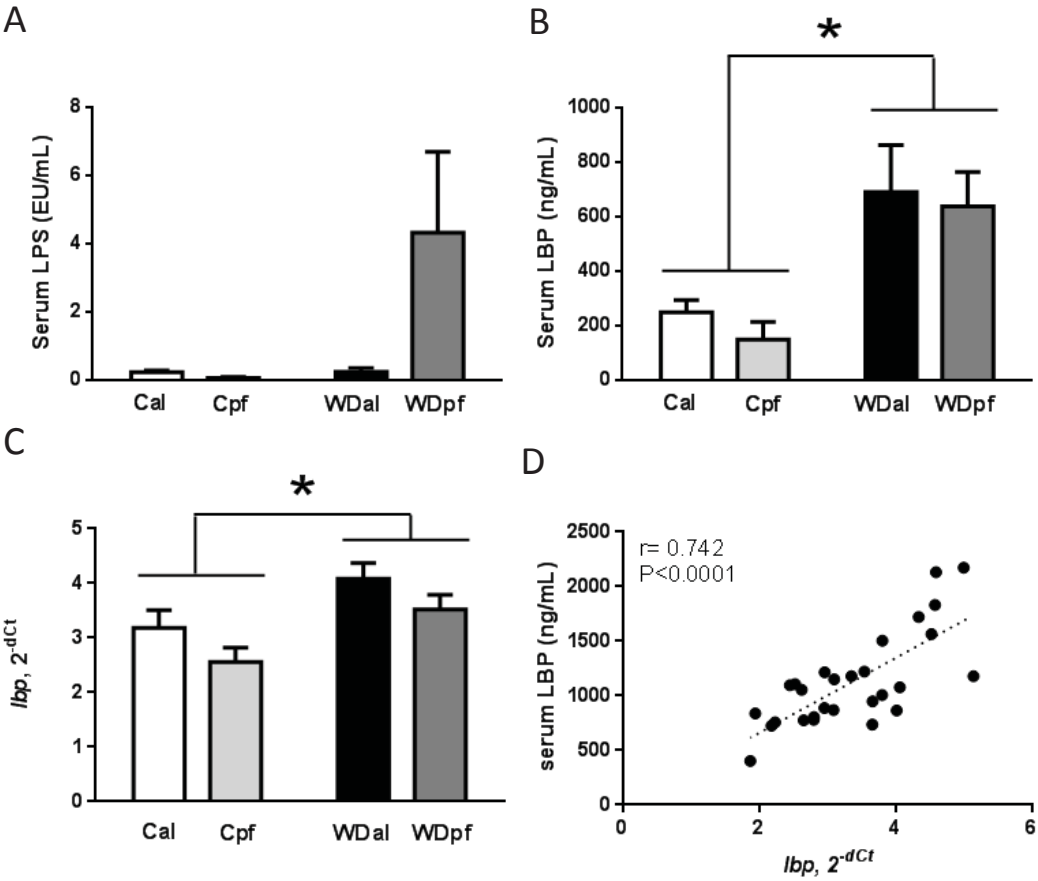
A
Serum LPS (EU/mL)
8
6
4
2
0
Cal
Cpf
WDal
WDpf
B
*
Serum LBP (ng/mL)
1000
800
600
400
200
0
Cal
Cpf
WDal
WDpf
C
*
lbp, 2-dCt
5
4
3
2
1
0
Cal
Cpf
WDal
WDpf
D
serum LBP (ng/mL)
2500
2000
1500
1000
500
0
r= 0.742
P<0.0001
0
2
4
6
lbp, 2-dCt

FIGURE 3

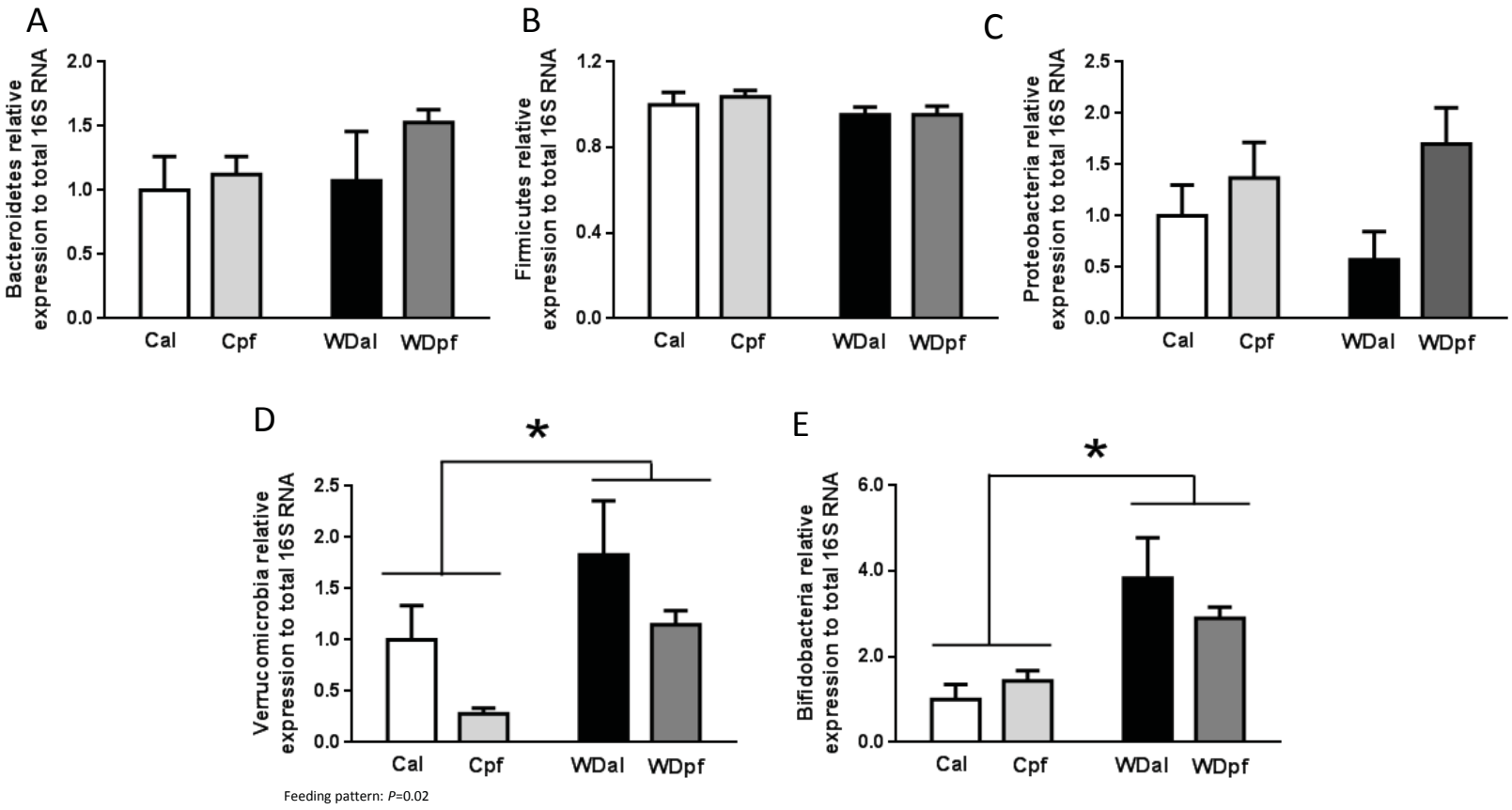
A
Bacteroidetes relative expression to total 16S RNA
2.0
1.5
1.0
0.5
0.0
Cal
Cpf
WDal
WDpf
B
Firmicutes relative expression to total 16S RNA
1.2
0.8
0.4
0.0
Cal
Cpf
WDal
WDpf
C
Proteobacteria relative expression to total 16S RNA
2.5
2.0
1.5
1.0
0.5
0.0
Cal
Cpf
WDal
WDpf
D
*
Verrucomicrobia relative expression to total 16S RNA
2.5
2.0
1.5
1.0
0.5
0.0
Cal
Cpf
WDal
WDpf
Feeding pattern: P=0.02
E
*
Bifidobacteria relative expression to total 16S RNA
6.0
4.0
2.0
0.0
Cal
Cpf
WDal
WDpf

FIGURE 4

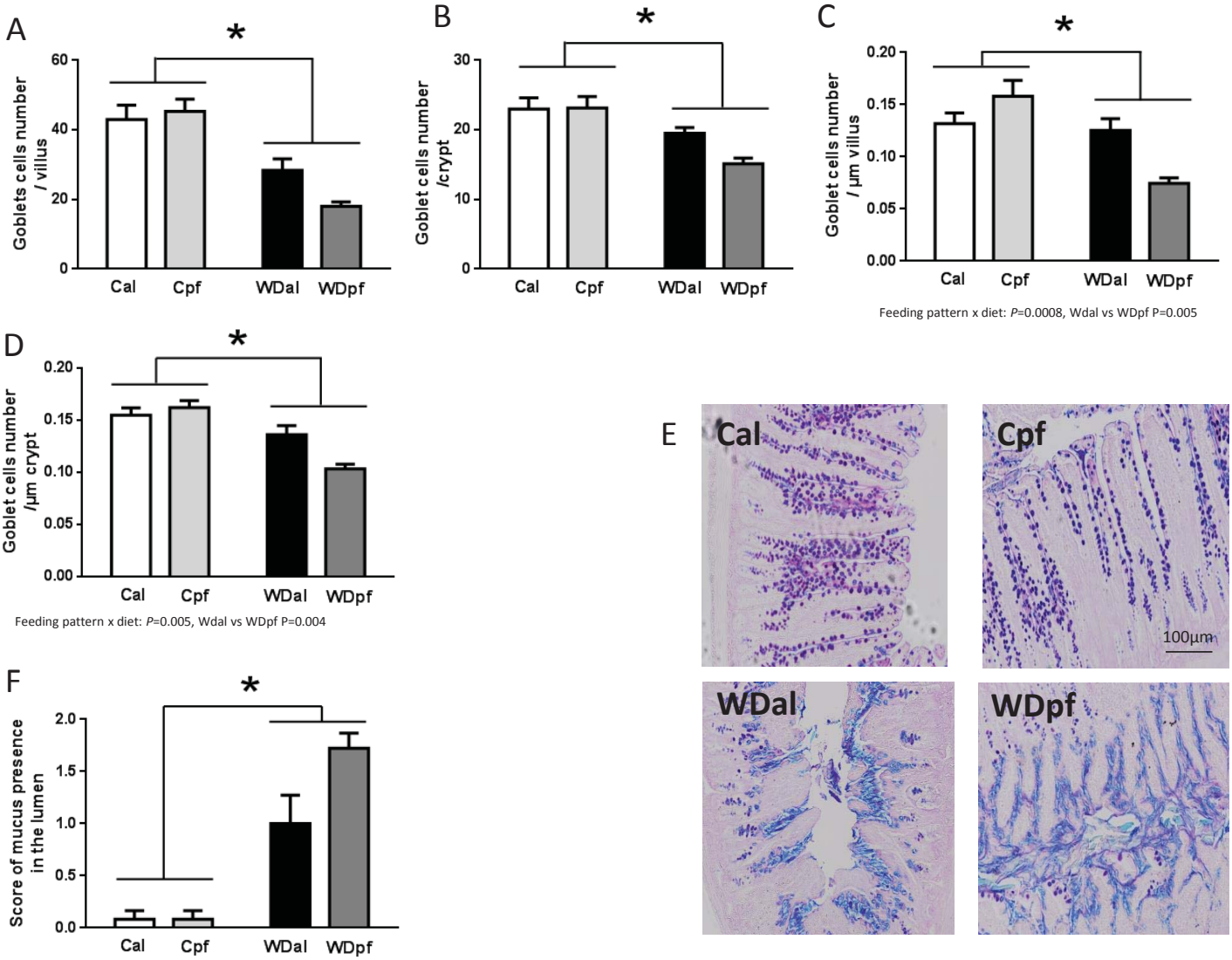
A
*
Goblets cells number / villus
60
40
20
0
Cal
Cpf
WDal
WDpf
B
*
Goblet cells number /crypt
30
20
10
0
Cal
Cpf
WDal
WDpf
C
*
Goblet cells number / µm villus
0.20
0.15
0.10
0.05
0.00
Cal
Cpf
WDal
WDpf
Feeding pattern x diet: P=0.0008, Wdal vs WDpf P=0.005
D
*
Goblet cells number /µm crypt
0.20
0.15
0.10
0.05
0.00
Cal
Cpf
WDal
WDpf
Feeding pattern x diet: P=0.005, Wdal vs WDpf P=0.004
E
Cal
Cpf
100µm
WDal
WDpf
F
*
Score of mucus presence in the lumen
2.0
1.5
1.0
0.5
0.0
Cal
Cpf
WDal
WDpf
Feeding pattern x diet: P=0.03, Wdal vs WDpf P=0.02

FIGURE 5

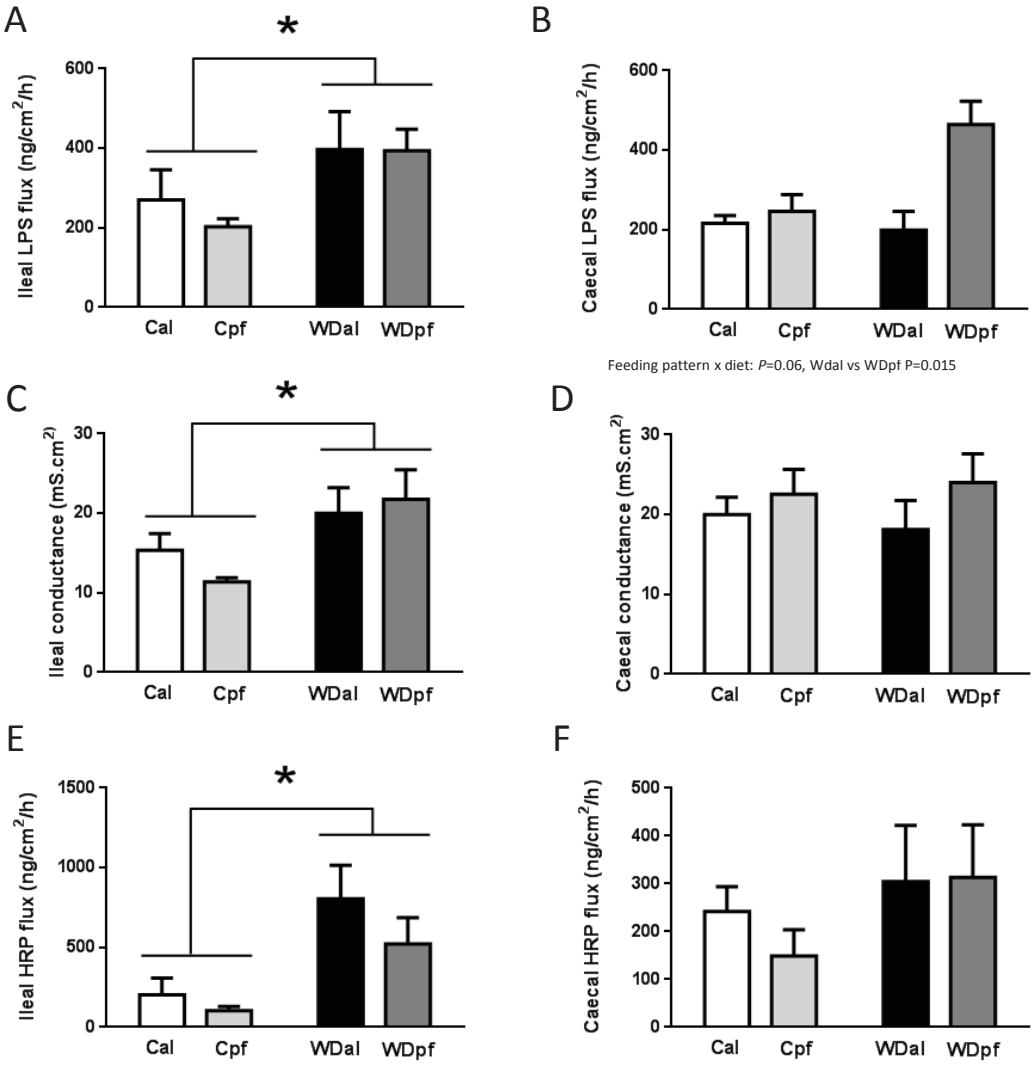
A
*
Ileal LPS flux (ng/cm2/h)
600
400
200
0
Cal
Cpf
WDal
WDpf
B
Caecal LPS flux (ng/cm2/h)
600
400
200
0
Cal
Cpf
WDal
WDpf
Feeding pattern x diet: P=0.06, Wdal vs WDpf P=0.015
C
*
Ileal conductance (mS.cm2)
30
20
10
0
Cal
Cpf
WDal
WDpf
D
Caecal conductance (mS.cm2)
30
20
10
0
Cal
Cpf
WDal
WDpf
E
*
Ileal HRP flux (ng/cm2/h)
1500
1000
500
0
Cal
Cpf
WDal
WDpf
F
Caecal HRP flux (ng/cm2/h)
500
400
300
200
100
0
Cal
Cpf
WDal
WDpf

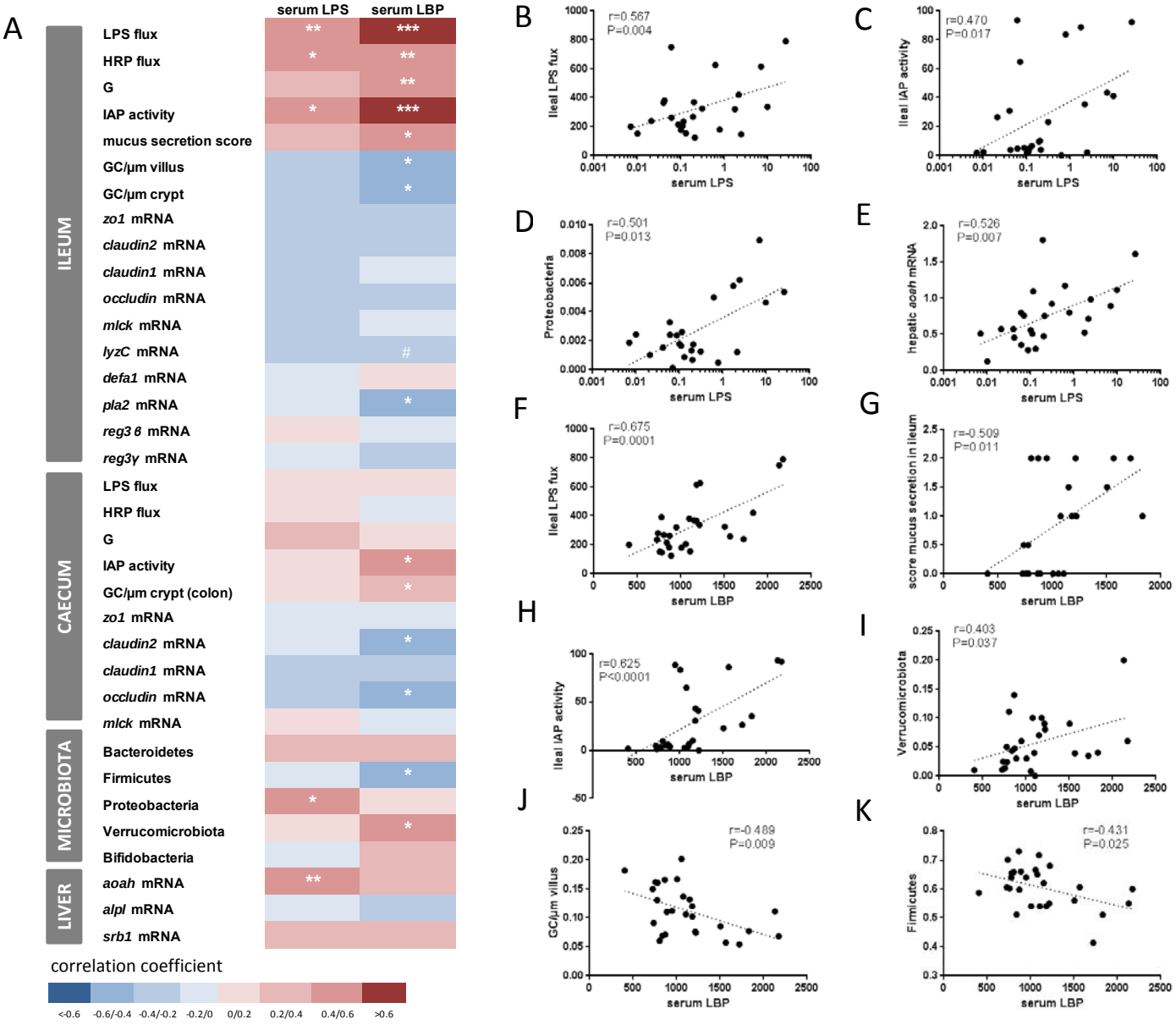
A
serum LPS
serum LBP
ILEUM
LPS flux
HRP flux
G
IAP activity
mucus secretion score
GC/µm villus
GC/µm crypt
zo1 mRNA
claudin2 mRNA
claudin1 mRNA
occludin mRNA
mlck mRNA
lyzC mRNA
defa1 mRNA
pla2 mRNA
reg3 δ mRNA
reg3γ mRNA
CAECUM
LPS flux
HRP flux
G
IAP activity
GC/µm crypt (colon)
zo1 mRNA
claudin2 mRNA
claudin1 mRNA
occludin mRNA
mlck mRNA
MICROBIOTA
Bacteroidetes
Firmicutes
Proteobacteria
Verrucomicrobiota
Bifidobacteria
LIVER
aoah mRNA
alpl mRNA
srb1 mRNA
correlation coefficient
<-0.6
-0.6/-0.4
-0.4/-0.2
-0.2/0
0/0.2
0.2/0.4
0.4/0.6
>0.6
B
r=0.567
P=0.004
Ileal LPS flux
serum LPS
C
r=0.470
P=0.017
Ileal IAP activity
serum LPS
D
r=0.501
P=0.013
Proteobacteria
serum LPS
E
r=0.526
P=0.007
hepatic aoah mRNA
serum LPS
F
r=0.675
P=0.0001
Ileal LPS fux
serum LBP
G
r=-0.509
P=0.011
score mucus secretion in ileum
serum LBP
H
r=0.625
P<0.0001
Ileal IAP activity
serum LBP
I
r=0.403
P=0.037
Verrucomicrobiota
serum LBP
J
r=-0.489
P=0.009
GC/µm villus
serum LBP
K
r=-0.431
P=0.025
Firmicutes
serum LBP

FIGURE 6

Table 1: Primers sequences used in this study

Gene	Forward (5'-3')	Reverse (3'-5')
ACTIN	CCCTAAGGCCAACCGTGAAA	CATACAGGGACAACACAGCCT
ALPL	GACATCGCCTATCAGCTAATGC	CCACATCAGTTCTGTTCTTGGG
AOAH	ATGAAGGCTGATGTGGTGTG	AGGACTTCCTGAGGACTTGT
BACTEROIDETES	ATACGCGAGGAACCTTACC	AGCTGACGACAACCATGCAG
BIFIDOBACTERIA	TCGCGTC(CT)GGTGTGAAAG	CCACATCCAGC(AG)TCCAC
DEFA1	AGAGGCAGAGGAAGAGACTAAA	AGGACTACAGGGCTCATCTAC
FIRMICUTES	TGAAACTYAAAGGAATTGACG	ACCATGCACCACCTGTC
GAPDH	GGTCGGTGTGAACGGATTT	TGGAAGATGGTGATGGGTTTC
HPRT1	TAGGTCCATTCCTATGACTGTAGA	TGGCCTGTATCCAACACTTC
IL-1β	ATCTATACCTGTCCTGTGTGATG	GACAGGTCTGTGCTCTGC
LBP	AGTCTGCAGAGAGAGCTGTA	CCAGGCTATGAAACTCGTACTG
LYZ-C	GAATGGGATGTCTGGCTACTATG	GTCTCCAGGGTTGTAGTTTCTG
PLA2gIIa	GCTGTGTGACTCATGACTGTT	CTCGGTAGGAGAACTTGTAGGT
PROTEOBACTERIA	AACGCGAAAAACCTTACCTACC	TGCCCTTTCGTAGCAACTAGTG
REG3-β	ATCACAGGTGCAAGGAGAAG	TGAAACAGGGCATAGCAGTAG
REG3-γ	GCATATGGCTCCTACTGCTATG	TCAGCTACATTGAGCACAGATAC
SCARB-1	GCAGTGATGATGGAGGACAA	GGGAACATGCCTGGGAAATA
UNIVERSAL 16S	AAACTCAAAKGAATTGACGG	CTCARRCACGAGCTGAC
VERRUMICROBIOTA	TCAKGTCAGTATGGCCCTTAT	CAGTTTTYAGGATTTCCTCCGCC

Table 2: IL-1β gene expression in ileum, caecum and liver after 6-week WD or C feeding.

					P-value		
	Cal	**Cpf**	**WDal**	**WDpf**	*diet*	*FP*	*diet x FP*
ileum, 2-^{dCt}	0.19 ± 0.06	0.19 ± 0.02	0.18 ± 0.02	0.22 ± 0.03	*0.85*	*0.53*	*0.65*
caecum, 2-^{dCt}	0.52 ± 0.24	0.64 ± 0.25	0.92 ± 0.46	0.91 ± 0.36	*0.009*	*0.69*	*0.58*
liver, 2-^{dCt}	0.11 ± 0.02	0.06 ± 0.01	0.11 ± 0.01	0.13 ± 0.03	*0.23*	*0.55*	*0.17*

Results are means ± SEM. FP=feeding pattern.

Table 3: IAP activity in ileum and caecum and anti-microbial peptides gene expression in ileum

					P-value		
	Cal	**Cpf**	**WDal**	**WDpf**	*Diet*	*FP*	*Diet x FP*
Ileal IAP activity (AU/mg)	4.4 ± 0.7	2.6 ± 0.5	51.1 ± 14.1	36.5 ± 10.2	*0.008*	*0.44*	*0.55*
Caecal IAP activity (AU/mg)	3.1 ± 0.6	3.2 ± 1.0	15.5 ± 2.7	10.2 ± 1.8	*<0.0001*	*0.21*	*0.19*
reg3-β, 2^{-dCt}	0.42 ± 0.16	0.18 ± 0.05	0.06 ± 0.02	0.11 ± 0.03	*0.009*	*0.24*	*0.08*
reg3-γ, 2^{-dCt}	0.34 ± 0.13	0.19 ± 0.03	0.08 ± 0.04	0.08 ± 0.0	*0.003*	*0.19*	*0.18*
lyzc, 2^{-dCt}	0.02± 0.005	0.12 ± 0.02	0.03 ± 0.008	0.08 ± 0.03	*0.58*	*0.009*	*0.29*
defa-1,2^{-dCt}	0.46 ± 0.11	0.52 ± 0.06	0.67 ± 0.16	0.49 ± 0.05	*0.33*	*0.48*	*0.20*
pla-2,2^{-dCt}	0.01 ± 0.004	0.08 ± 0.02	0.01 ± 0.002	0.04 ± 0.01	*0.11*	*0.001*	*0.13*

Results are means ± SEM. FP=feeding pattern.

Table 4: Tight junction protein and MLCK gene expression in ileum and caecum

					P-value		
	Cal	**Cpf**	**WDal**	**WDpf**	*Diet*	*FP*	*Diet x FP*
Ileum							
zo-1, 2^{-dCt}	0.60 ± 0.04	1.50 ± 0.13	0.56 ± 0.02	1.24 ± 0.26	*0.62*	*0.002*	*0.52*
claudin-1,2^{-dCt}	0.59 ± 0.11	1.47 ± 0.17	0.98 ± 0.34	1.56 ± 0.35	*0.46*	*0.04*	*0.68*
claudin-2, 2^{-dCt}	0.69 ± 0.12	1.72 ± 0.17	0.76 ± 0.06	1.30 ± 0.39	*0.61*	*0.02*	*0.46*
occludin, 2^{-dCt}	0.35 ± 0.05	0.97 ± 0.06	0.40 ± 0.01	0.86 ± 0.16	*0.82*	*0.0009*	*0.60*
mlck, 2^{-dCt}	0.003 ± 0.001	0.004 ± 0.001	0.003 ± 0.001	0.005 ± 0.001	*0.61*	*0.03*	*0.69*
Caecum							
zo-1, 2^{-dCt}	0.79 ± 0.13	1.31 ± 0.15	0.87 ± 0.10	1.25 ± 0.22	*0.96*	*0.03*	*0.71*
claudin-1,2^{-dCt}	0.02 ± 0.004	0.03 ± 0.003	0.03 ± 0.004	0.04 ± 0.01	*0.28*	*0.19*	*0.51*
claudin-2, 2^{-dCt}	0.14 ± 0.008	0.31 ± 0.02	0.09 ± 0.01	0.22 ± 0.05	*0.07*	*0.001*	*0.53*
occludin, 2^{-dCt}	5.48 ± 1.13	5.76 ± 0.34	3.33 ± 0.20	3.98 ± 0.40	*0.003*	*0.44*	*0.75*
mlck, 2^{-dCt}	2.00 ± 0.3	2.62 ± 0.27	1.92 ± 0.31	2.8 ± 0.27	*0.87*	*0.02*	*0.65*

Results are means ± SEM. FP=feeding pattern

Table 5 : Hepatic detoxification enzymes and receptors gene expression

					P-value		
	Cal	**Cpf**	**WDal**	**WDpf**	*Diet*	*FP*	*Diet xFP*
aoah, 2^{-dCt}	0.60 ± 0.08	0.61 ± 0.15	0.72 ± 0.07	0.84 ± 0.14	*0.24*	*0.63*	*0.70*
alpl, 2^{-dCt}	0.14 ± 0.02	0.27 ± 0.05	0.13 ± 0.02	0.18 ± 0.03	*0.17*	*0.01*	*0.29*
scarb-1, 2^{-dCt}	0.90 ± 0.13	0.63 ± 0.10	0.99 ± 0.11	0.82 ± 0.09	*0.19*	*0.05*	*0.64*

Results are means ± SEM. FP=feeding pattern.